Free Radical Biology and Medicine 188 (2022) 71–82

Contents lists available at ScienceDirect

Free Radical Biology and Medicine

journal homepage: www.elsevier.com/locate/freeradbiomed

Cyanidin and delphinidin restore colon physiology in high fat diet-fed mice: Involvement of TLR-4 and redox-regulated signaling

Dario E. Iglesias [a,b,1], Eleonora Cremonini [a,b,1], Shelly N. Hester [c], Steven M. Wood [c], Mark Bartlett [c], Cesar G. Fraga [a,d,e], Patricia I. Oteiza [a,b,*]

[a] Department of Nutrition, University of California, Davis, CA, USA
[b] Department of Environmental Toxicology, University of California, Davis, CA, USA
[c] Pharmanex Research, NSE Products, Inc., Provo, UT, USA
[d] Physical Chemistry, School of Pharmacy and Biochemistry, Universidad de Buenos Aires, Buenos Aires, Argentina
[e] Instituto de Bioquímica y Medicina Molecular-Dr. Alberto Boveris (IBIMOL), UBA-CONICET, Buenos Aires, Argentina

ARTICLE INFO

Keywords:
Cyanidin
Delphinidin
Endotoxemia
High fat diet
Tight junctions
Colon physiology

ABSTRACT

Consumption of high fat diets (HFD) mimics a modern or "Western style" diet pattern and can impair intestinal barrier integrity, leading to endotoxemia and associated unhealthy conditions. This study investigated if supplementation with an anthocyanin (cyanidin and delphinidin glucosides)-rich extract (CDRE) could revert or mitigate HFD-induced alterations of colonic physiology in part through the regulation of Toll-Like Receptor 4 (TLR-4)- and redox-regulated signaling. C57BL/6J male mice were fed for 4 weeks with a control or an HFD. Then, mice were divided in four groups fed either control or HFD, or these diets supplemented with CDRE for the subsequent 4 weeks. After 8 weeks on the HFD we observed in the colon: i) disruption of tight junction structure and function; ii) increased TLR-4 expression; iii) increased NADPH oxidase NOX1 expression, and iv) activation of redox-sensitive and TLR-4-triggered pathways, i.e. NF-κB, ERK1/2, JNK1/2, PI3K/Akt. All these events were prevented or reverted by CDRE supplementation. Supporting the relevance of CDRE-mediated downregulation of TLR-4 on its colon beneficial effect; *in vitro* (Caco-2 cell monolayers), cyanidin, delphinidin and their metabolites protocatechuic and gallic acid, mitigated lipopolysaccharide (LPS)-induced monolayer permeabilization by restoring tight junction structure and dynamics and preventing lipid/protein oxidation. The CDRE also mitigated HFD-mediated alterations in parameters of goblet cell differentiation and function, including the downregulation of markers of goblet cell differentiation (Klf4), and intestinal mucosa healing (Tff3). Results show that a short-term supplementation with cyanidin and delphinidin, protect from HFD-induced alterations in colon physiology in part through the modulation of TLR-4- and redox-regulated signaling.

1. Introduction

Preservation of the structure and function of the gastrointestinal (GI) tract is central to sustained health. Increasing evidence links GI tract dysfunction to the adverse consequences of consuming Western-style diets, and the frequently concomitant obesity [1]. In particular, high fat diets (HFD) cause intestinal inflammation, barrier permeabilization, dysbiosis, and affect several other aspects of GI immunity [2–6]. Thus, the action of select bioactives to prevent or mitigate the adverse GI tract effects of unhealthy diets would have direct benefits on human systemic and metabolic health [4,7].

The GI barrier regulates interactions among resident immune cells, the luminal content, the GI microbiota, and the host [8]. Intestinal permeabilization is central in the development of HFD- and

Abbreviations: 4-HNE, 4-hydroxynonenal; AC, anthocyanidins; CDRE, anthocyanin (cyanidin and delphinidin glycosides)-rich extract; ERK1/2, extracellular signal-regulated kinase; GI, gastrointestinal; HFD, high fat diet; IKK, IκB kinase; JNK, c-Jun N-terminal kinase; Klf4, Krüppel-like factor 4; LBP, LPS-binding protein; LPS, lipopolysaccharide; MCP-1, monocyte chemoattractant protein-1; MyD88, myeloid differentiation primary response 88; MLC, myosin light chain; MLCK, MLC kinase; MLCP, MLC phosphatase; Muc2, mucin 2; NAFLD, non-alcoholic fatty liver disease; iNOS, inducible nitric oxide synthase; NOX, NADPH oxidase; PI3K, phosphoinositide 3-kinase; Tff3, trefoil factor 3; TJ, tight junction; TLR, Toll-like receptor; TNFα, tumor necrosis factor alpha; T2D, type 2 diabetes.

* Corresponding author. Departments of Nutrition University of California, Davis, CA, USA.
E-mail address: poteiza@ucdavis.edu (P.I. Oteiza).

[1] Equally contributed.

https://doi.org/10.1016/j.freeradbiomed.2022.06.006
Received 11 May 2022; Received in revised form 31 May 2022; Accepted 7 June 2022
Available online 9 June 2022

obesity-associated diseases [4–6,9]. Gut barrier function is sustained by a protein complex, the tight junction (TJ), that links neighboring epithelial cells. While regulating the transport of water and ions, TJs prevent the paracellular passage of luminal food and microbiota toxins into the circulation. A disrupted barrier allows the paracellular passage of luminal bacterial lipopolysaccharides (LPS) to blood, resulting in metabolic endotoxemia and initiating systemic inflammation. In terms of mechanisms, consumption of HFD causes the intestinal upregulation of NADPH oxidases NOX1 and NOX4, the activation of the redox sensitive mitogen activated kinase (MAPK) ERK1/2 and transcription factor NF-κB, which trigger the opening of the TJs [10,11]. These cascades are also activated by LPS through its interaction with Toll-Like Receptor (TLR)-4, then feeding a cycle of local inflammation, oxidative stress, and further barrier permeabilization. In parallel, HFD affect goblet cells with additional adverse consequences for GI immune protection [2,12,13].

Flavonoids are a large family of bioactive molecules that can modulate GI tract function, and through such actions, sustain health [14]. Given differences in chemical structure and metabolism, these compounds differ in how they affect the GI tract. Among flavonoids, compounds belonging to the anthocyanidin (AC) subfamily have been shown to have GI anti-inflammatory and/or barrier protective effects both *in vitro* [10,15–18] and in rodent models of HFD-induced obesity [4,19] and inflammatory bowel diseases [20]. Supplementation for 14 weeks with cyanidin and delphinidin prevented HFD-induced intestinal permeabilization, endotoxemia, altered mucus secretion, and altered microbiota profiles in mice [4]. The capacity of these AC to protect the intestinal barrier from HFD-associated and inflammation-induced increased barrier permeability have been attributed to the regulation of epithelial cell redox homeostasis and signaling, as well as to the preservation of TJs [4,10]. Importantly, the capacity of flavonoids, and AC in particular, to mitigate the adverse GI tract effects of HFD can contribute to mitigate the adverse consequences of Western style diets on systemic and metabolic health, including insulin resistance and steatosis [4,7].

We recently observed that short-term supplementation (4 weeks) with a cyanidin- and delphinidin-rich extract (CDRE) in HFD-fed mice prevented endotoxemia and the liver activation of proinflammatory signaling pathways downstream of the TLR-4 [21]. This could be due to AC-mediated preservation of intestinal barrier function. We now investigated if CDRE supplementation could mitigate the adverse consequences of a HFD on colon barrier and goblet cell physiology. The involvement of TLR-4- and redox-regulated signaling pathways on AC-mediated preservation of TJ structure and dynamics was characterized in mice and Caco-2 cells.

2. Materials and methods

2.1. Materials

Antibodies for IκB kinase (IKK) α (#2682), phospho (Ser176/180)-IKKα/β (#2697), p65 (#8242), phospho (Ser536)-p65 (#3033), TLR-2 (#13744), phospho (Thr180/Tyr182)-p38 (#9211), extracellular signal-regulated kinase (ERK1/2) (#9102), phospho (Thr202/Tyr204)-ERK1/2 (#4370), c-jun N-terminal kinase (JNK) 2 (#9258), PI3K (#5405), phospho (Ser473)-Akt (#4060), Akt (#9279), myosin light chain (MLC) (#8505), phospho (Thr18/Ser19)-MLC (#3674), MyD88 (#4283), myosin phosphatase target subunit 1 (MYPT1) (#8574), phospho (Thr696)-MYPT1 (#5163), and β-actin (#12620) were obtained from Cell Signaling Technology (Danvers, MA). Antibodies for TLR-4 (sc-293072), nitric oxide synthase 2 (iNOS) (sc-649), phospho (Thr183/Tyr185)-JNK1/2/3 (sc-6254) and HSC-70 (sc-1059) were from Santa Cruz Biotechnology (Santa Cruz, CA). Antibodies for 4-hydroxynonenal (4-HNE) (ab46545), NADPH oxidase (NOX) 1 (ab55831), NOX4 (ab216654) and $gp91_{phox}$ (ab129068) and kits to measure concentrations of free fatty acids and LPS-binding protein (LBP) were purchased from Abcam, Inc. (Cambridge, MA). Antibodies for ZO-1 (33–9100), occludin (33–1500), claudin-1 (71–7800), MLC kinase (MLCK) (PA5-15176), phospho (Thr18/Ser19)-MLC (PIPA5117239), and the Periodic Acid Schiff (PAS) solution were obtained from Thermo Fisher Scientific Inc. (Piscataway, NJ). PVDF membranes and Clarity Western ECL Substrate were obtained from Bio-Rad (Hercules, CA). 3-(4,5-dimethylthiazol-2-yl)-2,5-diphenyltetrazolium bromide (MTT) and all other chemicals were purchased from Sigma-Aldrich Co (St. Louis, MO). The CDRE was provided by NSE Products, Inc. (Provo, UT) and its chemical composition was included in a previous publication [21].

2.2. Animals and animal care

All procedures were in agreement with standards for care of laboratory animals as outlined in the NIH Guide for the Care and Use of Laboratory Animals. Experimental protocols were approved before implementation by the University of California, Davis Animal Use and Care Administrative Advisory Committee. Procedures were administered under the auspices of the Animal Resource Services of the University of California, Davis.

As summarized in Fig. 1A, sixty mice (male C57BL/6J, 20–25 g), purchased from the Jackson Laboratories (Sacramento, CA), were acclimated for one week to the control diet and subsequently fed for 4 weeks with: i) a diet containing approximately 10% total calories from fat (Control, C group); or ii) a diet containing approximately 60% total calories from fat (lard) (HF group) [22]. After 4 weeks on the diets, 10 mice per group were euthanized and the 20 remaining in each group were divided in two subgroups (10 mice/subgroup) that either continued on the control or the high fat diets, or were supplemented with CDRE to receive 50 mg of cyanidinin and delphinidin, 28.9 and 21.1 mg, respectively/kg body weight for 4 weeks (control diet supplemented with CDRE, CA group; HFD supplemented with CDRE, HFA group).

At week 2, a blood sample (20 μl) was collected from the submandibular vein. At weeks 4 and 8, mice were euthanized by cervical dislocation, and blood was collected from the sub-mandibular vein. Blood samples were collected into EDTA tubes, and plasma was obtained after centrifugation at 3000×*g* for 15 min at room temperature. The colon was collected, measured and weighed, and subsequently sections were processed either for histology, or flash frozen in liquid nitrogen and then stored at −80 °C for further analysis.

2.3. LPS-binding protein assay

Plasma LPS-binding protein (LBP) levels were determined at 0, 2, 4 and 8 weeks on the dietary treatments, using a kit from Abcam (Cambridge, MA) following the manufacturer's protocols.

2.4. Histological analyses

The proximal colon samples were fixed overnight in 4% (w/v) neutralized paraformaldehyde solution. Samples were subsequently washed twice in phosphate buffer saline solution, dehydrated, and then embedded in paraffin for histological analysis. Sections (5 μm thickness) were obtained from paraffin blocks and placed on glass slides. Periodic Acid Schiff staining (PAS) was performed following standard procedures. 3 to 5 pictures/animal were taken and 10–12 crypts/picture were examined using a Leica DMI3000 B microscope (Leica Microsystems Inc., Buffalo Grove, IL), with a 20x ocular lens. Goblet cells number and crypts length were assessed and analyzed using NIH Image J software. The researchers were blinded to the identity of all samples.

2.5. Western blot analysis

Colon samples were homogenized as previously described [23] using a BeadMill24 (Thermo Fisher Scientific Inc., Piscataway, NJ). Aliquots of total homogenates containing 30–40 μg protein were denatured with

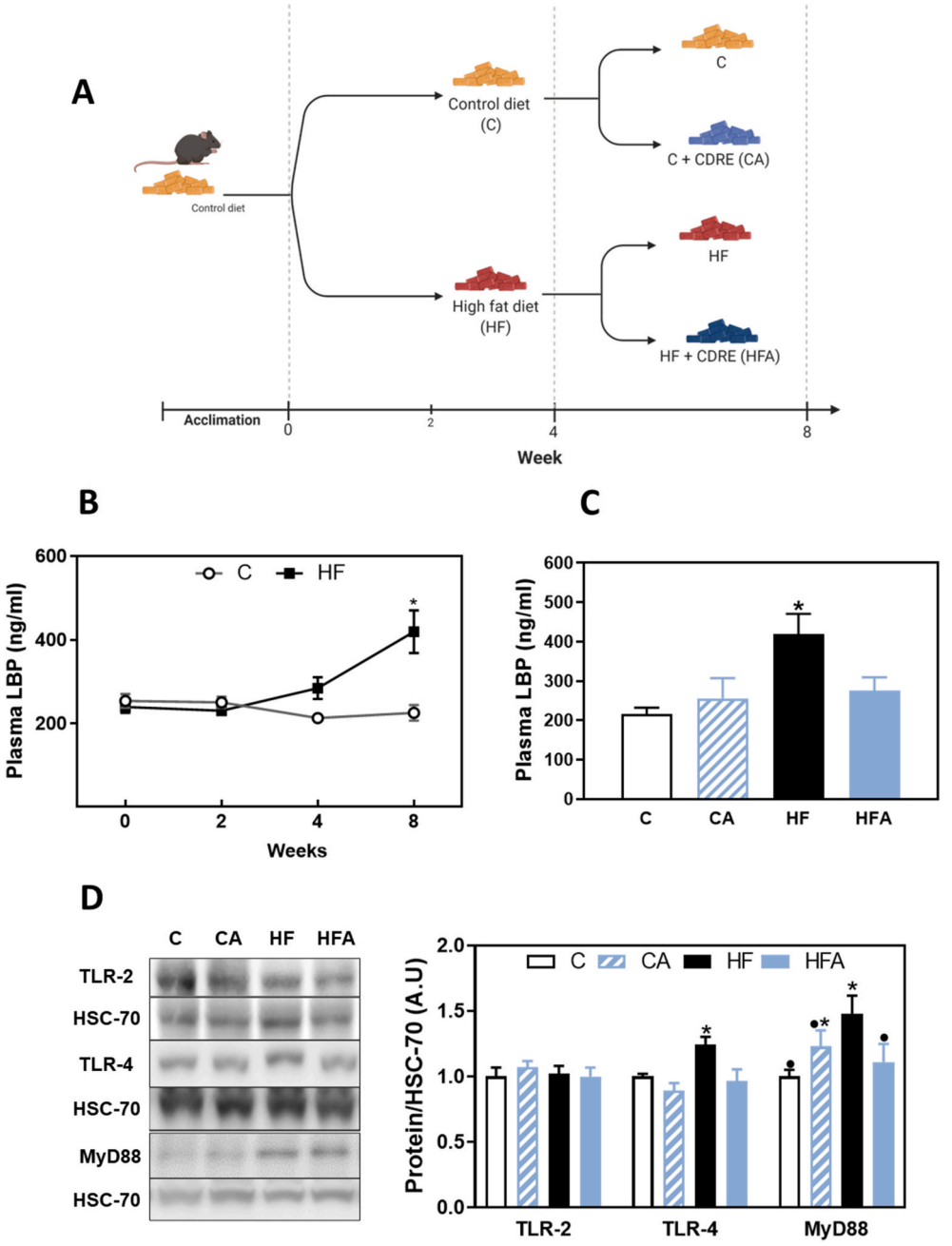

Fig. 1. Effects of the supplementation with CDRE on LPS-binding protein and on colon TLRs and MyD88 expression in mice fed control and high fat diets. A- Experimental design. **B-D-** At weeks 0, 2, 4, and/or 8 on the corresponding diets the following parameters were measured: **B,C-** Plasma LPS-binding protein (LBP) concentration. **B-** Kinetics of HFD-induced changes in plasma LBP, and **C-** Plasma LBP concentration at week 8. **D-** TLR-2, TLR-4, and MyD88 protein levels in the colon were measured by Western blot. Bands were quantified, values referred to HSC-70 levels (loading control) and results for CA, HF and HFA were referred to control group values (C). Results are shown as mean ± SE of 9–10 animals/group. **B-** *Significantly different ($p < 0.05$) from C at the corresponding time point; **C-***Significantly different compared to all other groups. **D-** Values having different symbols are significantly different ($p < 0.05$, one-way and two-ways ANOVA tests).

Laemmli buffer, separated by reducing 8–15% polyacrylamide gel electrophoresis, and electroblotted to PVDF membranes. Membranes were blocked for 5 min with EveryBlot blocking buffer (Bio-Rad, Hercules, CA), and subsequently incubated in the presence of the corresponding primary antibodies (1:750 or 1:1000 dilution) overnight at 4 °C. After incubation for 90 min at room temperature in the presence of secondary antibodies (HRP conjugated) (1:10,000 dilution), the conjugates were visualized using enhanced chemiluminescence. Images were captured using Bio-Rad ChemiDoc Imager, and bands were quantified using Image Lab Software (Bio-Rad, Hercules, CA).

2.6. RNA isolation and quantitative PCR (qPCR)

For quantitative PCR studies, RNA was isolated from the colon using TRIzol reagent (Invitrogen, Carlsbad, CA) following the manufacturers' instructions. cDNA was generated using high-capacity cDNA Reverse Transcriptase (Applied Biosystem, Grand Island, NY). mRNA levels of Klf4, Muc2, and Tff3 were assessed by quantitative PCR (iCycler, Bio-Rad, Hercules, CA) using the following primers:

Klf4: F: 5′-AGCCACCCACACTTGTGACTATG-3′
R: 5′-CAGTGGTAAGGTTTCTCGCCTGTG-3′
Muc2: F: 5′-CCATTGAGTTTGGGAACATGC-3′
R: 5′-TCGGCTCGGTGTTCAGAG-3′
Tff3: F: 5′-TAATGCTGTTGGTGGTCCTG-3′
R: 5′-CAGCCACGGTTGTTACACTG-3′
18S: F: 5′-AGTCCCTGCCCTTTGTACACA-3′
R: 5′-GATCCGAGGGCCTCACTAAAC-3′

The Ct values were normalized by the housekeeping gene 18S. Gene expression was determine using the $2^{-\Delta\Delta Ct}$ method [24].

2.7. Cell culture and incubations

Caco-2 cells were cultured at 37 °C and 5% (v/v) CO_2 atmosphere in minimum essential medium (MEM) supplemented with 10% (v/v) fetal bovine serum (FBS), antibiotics (50 U/ml penicillin and 50 μg/ml streptomycin), 1% (v/v) of 100X non-essential amino acids, and 1 mM sodium pyruvate. The medium was replaced every 3 days during cell growth and differentiation. Cells were used between passages 5 and 20.

For the experiments, cells were differentiated in inserts for 19–21 days and in dishes for 10–12 days. For experiments in dishes, cells were incubated for 72 h with LPS (100 ng/ml), in the absence or presence of 1 μM (poly)phenols cyanidin 3-*O*-glucoside, delphinidin 3-*O*-glucoside, protocatechuic acid (PCA) or gallic acid (GA). For experiments in inserts, Caco-2 cells were treated for 72 h with LPS (100 ng/ml) added at both the upper and lower chambers, in the absence or presence of 1 μM cyanidin 3-*O*-glucoside, delphinidin 3-*O*-glucoside, PCA or GA added to the upper chamber. All the experiments were performed in 2% (v/v) FBS and phenol red-free MEM and the media were replaced every 24 h.

2.8. Evaluation of Caco-2 monolayer permeability

Caco-2 monolayer permeability was evaluated by measuring the transepithelial electrical resistance (TEER) and the paracellular transport of FITC-dextran as previously described [10]. For both methods, the experiments were started when TEER values were between 350 and 450 Ω. cm^2 (19–21 d). For the evaluation of TEER and FITC-dextran permeability, Caco-2 cell monolayers were incubated for 72 h with LPS (100 ng/ml) and in the absence or the presence of the cyanidin-3-*O*-glucosides, delphinidin-3-*O*-glucosides, PCA or GA. LPS, the different anthocyanins and their metabolites were replaced daily. After 72 h incubation, TEER and the FITC-dextran permeability were evaluated. TEER was measured using a Millicell-ERS Resistance System (Millipore, Bedford, MA) that includes a dual electrode volt-ohm-meter. TEER was calculated as: TEER= (Rm – Ri) × A (Rm, transmembrane resistance; Ri, intrinsic resistance of a cell-free media; and A, the surface area of the membrane in cm^2). The apical-to-basolateral clearance of FITC-dextran (4 kDa) was calculated using the equation $f_{FITC}/(F_{FITC}/A)$, where f_{FITC} is the flux of FITC-dextran (in fluorescence units/h); F_{FITC}, the fluorescence of FITC-dextran in the upper compartment at zero time (in fluorescence units per nl); and A, the surface area of the membrane (1 cm^2). Arbitrary units (A.U.) were calculated based on TEER or apical-to-basolateral clearance values for the non-added (control) cells.

2.9. Cell viability

Cell viability was evaluated by the MTT assay, based on the conversion of MTT into formazan crystals by living cells. Cells were grown in 96-well plates for 10 days. Caco-2 cells were treated with LPS (100 ng/ml) for 72 h in the absence and the presence of the cyanidin-3-*O*-glucosides, delphinidin-3-*O*-glucosides, PCA or GA as previously described. After 72 h, 5 μl of the MTT solution (0.5 mg/ml in PBS) was added to 100 μl medium and incubated for 2 h at 37 °C. The reaction was stopped by addition of 100 μl of 0.01 N HCl containing 10% (w/v) SDS and plates were incubated overnight. Differences in absorbance (λ_{570}-λ_{690} nm) were determined using a Biotek Synergy H1 plate reader (BioTek Instruments, Winooski, VT) and normalized by values for the control (non-added) cells.

2.10. Evaluation of Caco-2 oxidant levels

Oxidant levels were estimated using the probe dihydroethidium (DHE). DHE enters cells, and when oxidized is converted into fluorescent compounds. Caco-2 cells were grown and differentiated in 96-well plates and treated with LPS (100 ng/ml) for 72 h as previously described. After incubation, the medium was removed, and cells were added with DHE (25 μM final concentration) and incubated for 30 min at 37 °C. After removal of DHE, cells were rinsed twice with PBS, added with 200 μl PBS and fluorescence was measured at λex: 535 nm; λem: 635 nm using a Biotek Synergy H1 plate reader (BioTek Instruments, Winooski, VT). To normalize fluorescence for the number of cells, DHE fluorescence values were referred to protein content measured with sulforhodamine B [25]. Values were normalized by those for the control (non-added) cells.

2.11. Statistical analysis

Data were analyzed by one-way analysis of variance (ANOVA) or Student's t-test using Statview 5.0 (SAS Institute Inc., Cary, NC). Fisher least significance difference test was used to examine differences between group means. For the LBP kinetic analysis, two-ways ANOVA was used to evaluate the experimental effects of time (0, 2, 4 and 8 weeks), treatment (C or HF), and any interaction between them. When significant differences were observed, the multiple comparison Tukey Honest Significant Difference (HSD) post-hoc was used to identify the differences between the mean. A p value < 0.05 was considered statistically significant. Data are shown as means ± SE.

3. Results

3.1. Effects of CDRE supplementation on HFD-induced endotoxemia and colonic TLR-2 and TLR-4 expression

As previously reported for this set of animals, after 8 weeks on the HFD mice developed obesity, insulin resistance and hyperlipidemia, which were not prevented by supplementation with the CDRE for the last 4 weeks [21]. An accepted marker of metabolic endotoxemia [19], LBP is a protein that binds LPS and delivers it to the soluble or membrane forms of C14 for subsequent binding to TLR-4. Plasma LPB levels showed a significant interaction between the C and the HF groups over time (0–8 weeks) ($p < 0.01$). Thus, as observed for plasma LPS [21], the plasma concentration of LBP was significantly higher (95%) in the HF group after 8 weeks on the HFD compared to the control group at the corresponding time points (Fig. 1B). Supplementation with the CDRE for the last 4 weeks on the HFD, attenuated the elevation of plasma LBP concentration triggered by HFD consumption (Fig. 1C).

Colonic TLR-4 and the downstream MyD88 protein levels were not significantly affected after 4 weeks on the HFD (Supplemental Fig. 1A). However, consistent with an increased exposure to LPS, after 8 weeks on the HFD, colonic TLR-4 and MyD88 levels were 24% and 48% higher, respectively, in the HF group compared to the C group. These increases were prevented by 4-week CDRE supplementation (Fig. 1D). Colon TLR-2 levels were not affected by the HFD consumption or CDRE supplementation.

3.2. Effects of CDRE supplementation on TJ structure and function

As shown in Fig. 3 for Caco-2 cell monolayers, exposure to high levels of LPS causes permeabilization which can be secondary to the upregulation TLR-4-triggered and redox-sensitive signals. Thus, we next investigated if the HFD affected parameters of colonic TJ structure and function. The expression of the TJ proteins occludin, ZO-1 and claudin-1 in the colon was evaluated by Western blot. After 4 weeks on the diets, we observed decreased levels of occludin, ZO-1 and claudin-1 (39, 33, and 52%, respectively) in HF compared to control mice (Fig. 2A). This decreased expression of TJ proteins was still observed after 8 weeks on the HFD. Thus, occludin, ZO-1 and claudin-1 protein levels were 29, 23 and 23% lower, respectively, in the HF group compared to the C group. CDRE supplementation for the last 4 weeks of the treatments restored occludin, ZO-1 and claudin-1 protein levels to control values (Fig. 2B).

TJ dynamics is regulated by MLCK, the kinase that phosphorylates MLC leading to TJ opening and increased paracellular permeability. MLCK expression and MLC phosphorylation were not affected after 4-

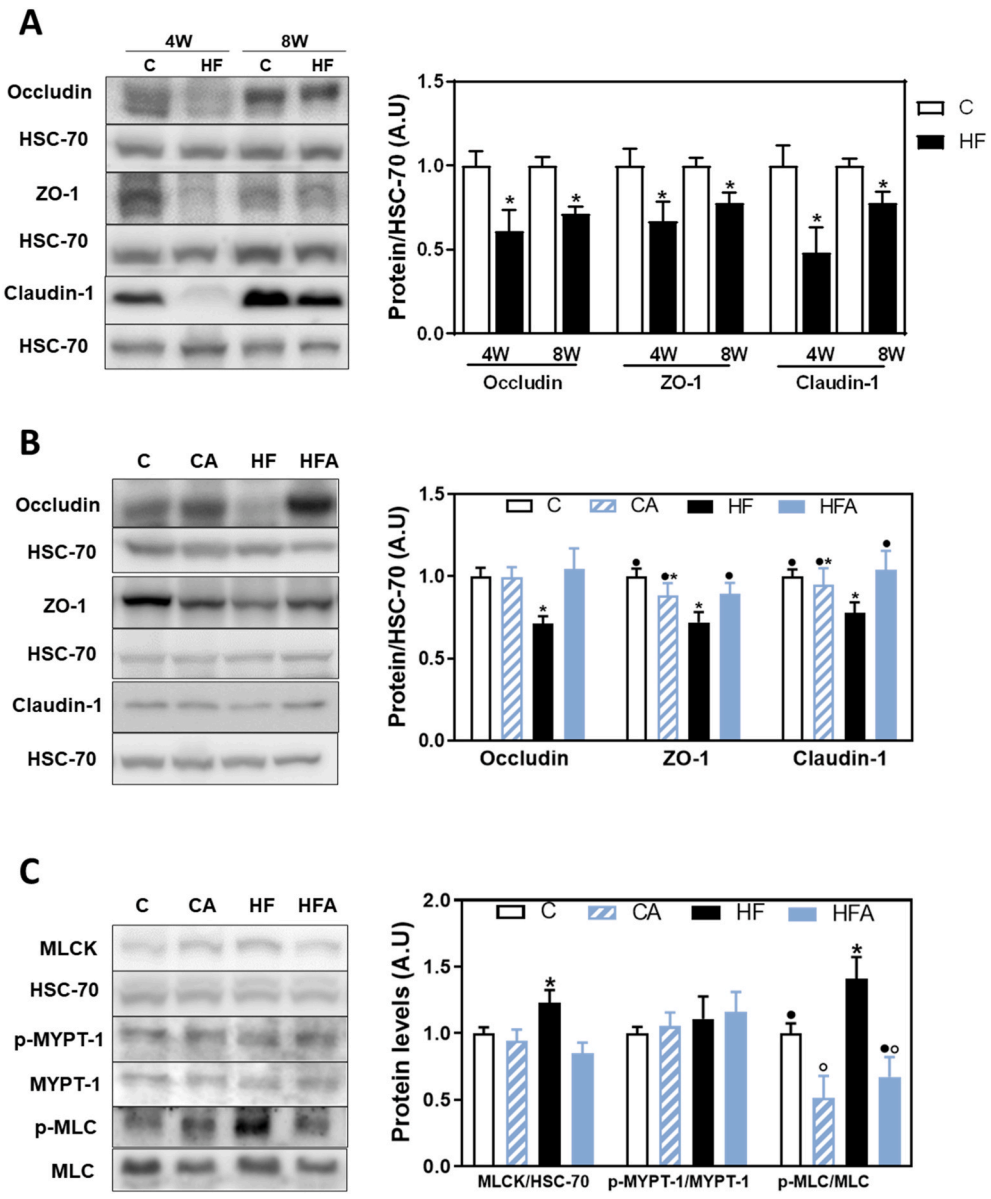

Fig. 2. Effects of the supplementation with CDRE on HFD-induced changes in tight junction proteins and events involved in TJ opening. Mice were fed the different diets as described in methods. **A, B-** After 4 and 8 weeks on the corresponding diets TJ protein levels, i.e. occludin, ZO-1 and claudin-1, were measured in the colon by Western blot. **C-** After 8 weeks of the corresponding diets MLCK expression, MYPT-1 (Thr696) and MLC (Thr18/Ser19) phosphorylation were assessed in the colon by Western blot. Bands were quantified and values for occludin, ZO-1, claudin-1 and MLCK referred to HSC-70 levels (loading control) or for MYPT-1 and MLC to total protein levels. Results for CA, HF and HFA were referred to control group values (C). Results are shown as mean ± SE of 9–10 animals/group. *Significantly different compared to other groups. Values having different symbols are significantly different ($p < 0.05$, one-way ANOVA test).

week of HFD consumption (Supplemental Fig. 2). After 8 weeks, the HFD caused a 23% and 41% increase in MLCK expression and MLC phosphorylation in Thr18/Ser19, respectively, that were both prevented by AC supplementation (Fig. 2C). We next evaluated the levels of phosphorylation of MYPT-1, a subunit of the enzyme MLC phosphatase (MLCP) that dephosphorylates MLC. Phosphorylation levels of MYPT-1 at Thr696 were not affected by the 8-week consumption of the HFD or CDRE supplementation (Fig. 2C).

3.3. Effects of 3-O-glucosides of cyanidin and delphinidin, protocatechuic acid and gallic acid on LPS-induced Caco-2 cell monolayer permeabilization

To evaluate if the regulation of LPS/TLR-4 is involved in AC prevention of barrier permeabilization we investigated the capacity of 3-*O*-glucosides of cyanidin and delphinidin, PCA and GA to prevent LPS-induced permeabilization of Caco-2 cell monolayers. We selected these compounds because both, the parent AC and their main microbiota metabolites, PCA and GA, are found in human colon and/or feces after consumption of the pure anthocyanins or anthocyanin-rich foods [26–29]. To initially determine the optimum incubation time for LPS to induce TJ alterations, cells were treated with LPS (100 ng/ml) for 24 to 96 h. Cells treated with LPS for 72 h showed a 29% decrease in occludin protein levels compared to non-added controls (Supplemental Fig. 3A). This treatment did not affect Caco-2 cell viability (Supplemental Fig. 3B). Both TEER and FITC-dextran paracellular transport were measured to evaluate monolayer permeability. Incubation for 72 h in the presence of LPS, added to the upper and lower chambers, caused a 22% decrease in TEER, and a 45% increase in FITC-dextran paracellular transport compared to non-added cells (Fig. 3A). Addition of 1 μM cyanidin-3-*O*-glucosides,delphinidin-3-*O*-glucosides, PCA and GA to the upper chamber prevented LPS-induced decreased TEER and increased FITC-dextran transport.

In agreement with the loss of barrier integrity, after 72-h incubation, LPS caused 27, 24 and 24% decrease in occludin, ZO-1 and claudin-1 protein levels, respectively (Fig. 3B). Both, cyanidin- and delphinidin-3-*O*-glucosides at 1 μM concentration were effective at preventing LPS-induced decrease in all TJ proteins tested. PCA (1 μM) inhibited the decreases observed in ZO-1 and claudin-1, but not that of occludin. GA (1 μM) treatment restored claudin-1 levels but did not prevent occludin and ZO-1 protein decreases.

The dynamics of the TJ can also be altered by LPS. In this regard,

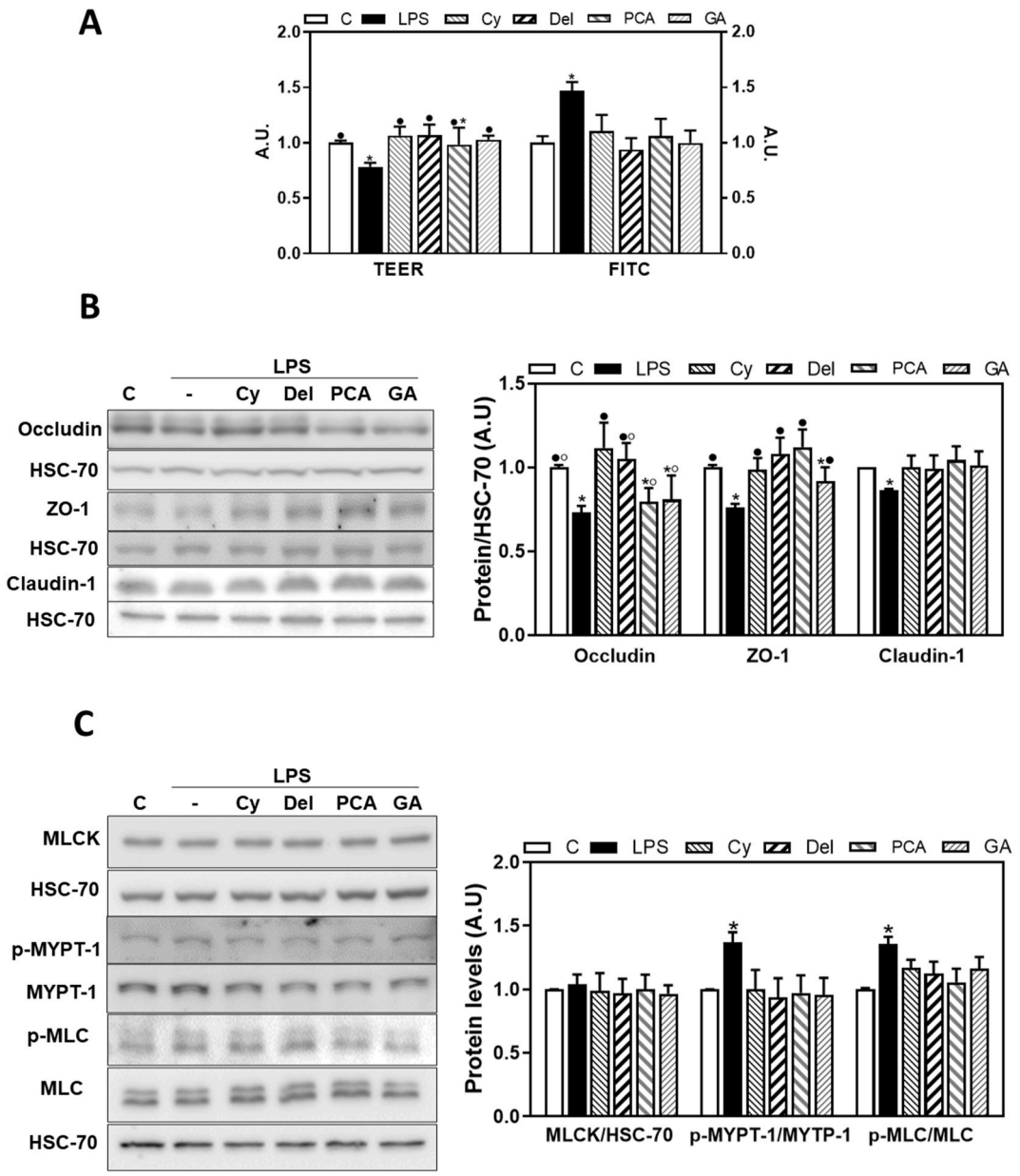

Fig. 3. Effects of 3-*O*-glucosides of cyanidin and delphinidin, and their metabolites, on LPS-induced permeabilization, TJ proteins levels and TJ regulatory events in Caco-2 cell monolayers. Caco-2 cells were treated with LPS for 72 h in the absence or the presence of 1 μM cyanidin- and delphinidin-3-*O*-glucosides, protocatechuic acid (PCA) and gallic acid (GA) as described in methods. **A-** Caco-2 cell monolayer permeability was evaluated by measuring TEER and FITC-dextran paracellular transport. We measured by Western blot: **B-** TJ protein levels (occludin, ZO-1 and claudin-1), and **C-** MLCK protein levels, MYPT-1 (Thr696) and MLC (Thr18/Ser19) phosphorylation. Bands were quantified and values for occludin, ZO-1, claudin-1 and MLCK referred to HSC-70 levels (loading control) and for MYPT-1 and MLC to total protein levels. *Significantly different compared to other groups. Results were referred to control, non-added cells values (C). Results are shown as mean ± SE of 9–10 independent experiments. Values having different symbols are significantly different ($p < 0.05$, one-way ANOVA test).

neither LPS nor the AC and their metabolites affected the expression of MLCK in Caco-2 cells (Fig. 3C). We did observe a significant increase (33%) in MLC phosphorylation levels after 72 h of incubation with LPS (Fig. 3C). This was associated with a 37% increase in phosphorylation levels of MYPT-1 at Thr696, which inhibits the phosphatase that dephosphorylates MLC. At 1 μM concentration, cyanidin 3-*O*-glucoside, delphinidin 3-*O*-glucoside, PCA and GA prevented LPS-induced increases in MYPT-1 and MLC phosphorylation.

Thus, the capacity of cyanidin and delphinidin and their metabolites to mitigate LPS-induced permeabilization can be in part due to the preservation of tight junction structure and to the inhibition of MLC phosphorylation.

3.4. Effects of 3-O-glucosides of cyanidin and delphinidin, protocatechuic acid and gallic acid on redox homeostasis in Caco-2 cells treated with LPS

Given the detrimental effects of LPS on the intestinal monolayer and the previously observed involvement of redox imbalance in the development of intestinal permeability [4,5,11,30], we next investigated the capacity of the cyanidin-3-*O*-glucosides, delphinidin-3-*O*-glucosides, PCA or GA, to modulate NOX1 expression and protein/lipid oxidative modifications in Caco-2 cells treated with LPS. We observed that 72 h incubation with LPS did not increase NOX1 protein expression, but caused a 33% increase in levels of 4-HNE-protein adducts (Fig. 4A). Cyanidin- and delphinidin-3-*O*-glucosides, PCA and GA, at 1 μM concentration, were effective at preventing LPS-induced increase of

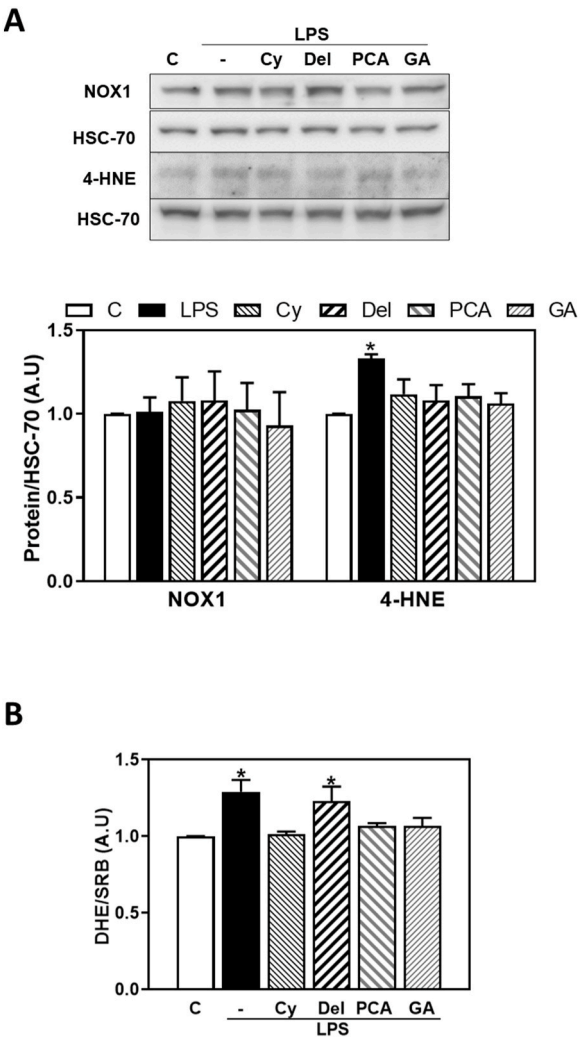

Fig. 4. Effects of 3-*O*-glucosides of cyanidin and delphinidin, and their metabolites, on parameters of oxidative stress in Caco-2 cell monolayers treated with LPS. Caco-2 cells were treated with LPS for 72 h in the absence or the presence of 1 μM cyanidin- or delphinidin-3-*O*-glucosides, protocatechuic acid (PCA) or gallic acid (GA) as described in methods. **A-** NOX1 and 4-HNE expression were evaluated by Western blot. **B-** Oxidation of the fluorescent probe DHE was assessed as described in methods. Bands for NOX1 and 4-HNE were quantified and values were referred to HSC-70 levels (loading control). DHE (oxidized DHE) fluorescence was normalized to sulforhodamine B (SRB) absorbance. Results were referred to control, non-added cells values (C). Results are shown as mean ± SE of 9–10 independent experiments. *Significantly different compared to other groups ($p < 0.05$, one-way ANOVA test).

4-HNE-protein adducts. Oxidative damage to cellular components could be due to increased production of oxidants. Thus, we next assessed the oxidation of the DHE probe in Caco-2 cells treated with LPS. After 72 h incubation, we observed a 30% increase in DHE oxidation compared to the non-added (control) cells. Cyanidin-3-*O*-glucoside, PCA, and GA, but not delphinidin-3-*O*-glucoside, mitigated LPS-induced increase of DHE oxidation (Fig. 4B).

3.5. Effects of CDRE supplementation on HFD-induced activation of signaling cascades downstream TLR-4

Upregulation of TLR-4 can be associated to the downstream activation of PI3K/Akt, NF-κB and the MAPKs. These signaling cascades are involved in the modulation of intestinal TJ function. After 4 weeks on the HFD, we did not observe changes in the activation of PI3K/Akt, p65, ERK1/2 and JNK1/2 (Supplemental Figs. 1B–D). However, all these pathways were activated after 8 weeks on the HFD. Thus, PI3K protein levels, and downstream Akt phosphorylation in Ser473 were 26% and 33% higher, respectively, in the HF compared to the C group (Fig. 5A). Both events were prevented by CDRE supplementation. We next evaluated IKK and p65 phosphorylation as parameters of activation of the NF-κB pathway. After 8 weeks on the HFD, IKK phosphorylation at Ser176/180 and p65 phosphorylation at Ser536 were 37% and 41% higher, respectively, in mice consuming the HFD compared to controls (Fig. 5B). These changes were prevented by CDRE supplementation. Among the MAPKs, ERK1/2 and JNK1/2 but not p38 were found to be activated in the colon by 8 weeks HFD consumption. Thus, ERK1/2 phosphorylation at Thr202/Tyr204 and JNK1/2 phosphorylation at Thr183/Tyr185 were 38% and 31% higher, respectively, in the HF group compared to the C group (Fig. 5C). CDRE supplementation fully prevented these increases.

3.6. Effects of CDRE supplementation and the HFD on parameters of redox homeostasis

We next evaluated changes in cell redox homeostasis. Thus, we assessed the expression of enzymes involved in $O_2^{\cdot-}$, H_2O_2 and NO production, i.e. NADPH oxidases and iNOS. Among these enzymes, only NOX1 protein levels were higher (55%) in the HF group compared to controls after 8 weeks on the HFD, which was prevented by CDRE supplementation (Fig. 6). No increase in NOX1 expression was observed after 4 weeks on the HFD (Supplemental Fig. 1E). NOX2, an isoform abundant in macrophages while negligible in epithelial cells, was not affected by the HFD or CDRE supplementation. This is in agreement with a lack of effect of the HFD on the levels of the macrophage marker F4/80 (data not shown). In control diet-fed mice, CDRE supplementation caused a significant decrease (34%) in NOX2 protein levels.

In terms of oxidative damage to cellular components, 4-HNE-protein adducts, which reflect both lipid and protein oxidation, were not affected in the colon by 8 weeks HFD consumption and/or by CDRE supplementation (Fig. 6).

3.7. CDRE supplementation prevents HFD-mediated alterations in colon morphology and disruption of goblet cells

Consumption of HFD can cause alterations in colon morphology. This was confirmed by evaluating the ratio colon weight/colon length, an indicator of tissue inflammation, and the length of the colon crypts. Consumption of the HFD caused a significant increase (16 and 12% at 4 and 8 weeks, respectively) in the colon weight/colon length ratio, and a decrease (19% at both time points) in crypt length (Fig. 7A and B). CDRE supplementation for 4 weeks restored these values to those of control mice.

Goblet cells are critical players in the preservation of barrier function. Consumption of HFD altered goblet cells number and parameters of goblet cell function. Thus, mice fed a HFD for 4 and 8 weeks showed a 19 and 23% decrease, respectively, in the number of goblet cells per crypt compared to control animals as measured by histological analysis after PAS staining (Fig. 7C–E). Supplementation with the CDRE restored the number of goblet cells in HFD-fed mice. We next evaluated the mRNA levels of markers of goblet cell differentiation (Krüppel-like factor 4, Klf4), mucin production (Muc2), and intestinal mucosa healing (Trefoil factor 3, Tff3) by qPCR. After 4 weeks on the HFD, no significant changes were observed in their mRNA levels (Fig. 7F). At 8 weeks, Klf4 mRNA levels were significantly lower (33%) in HFD-fed mice compared to control mice, this decrease was prevented by CDRE supplementation (Fig. 7F). While the HFD did not significantly affect Muc2 RNA levels at 4 and 8 weeks, supplementation with CDRE led to 64% higher mRNA levels of Muc2 compared to those in the HF group (Fig. 7F). After 8 weeks on the HFD, Tff3 mRNA levels were significantly lower (57%) in the HF than in the C group. Supplementation with CDRE not only mitigated the HFD-induced downregulation of Tff3 mRNA levels but

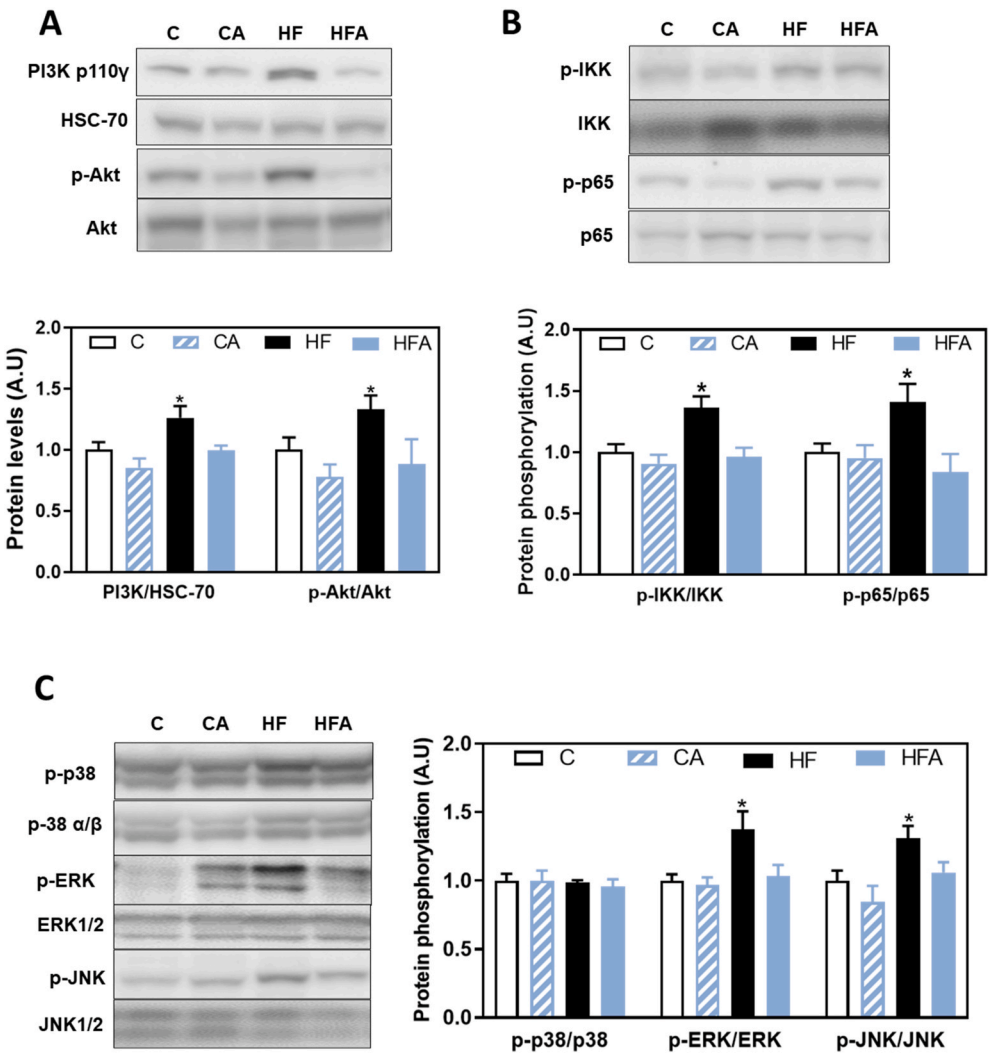

Fig. 5. Effects of the supplementation with CDRE on PI3K/Akt, NF-κB and MAPK pathways in the colon of mice fed a HFD. Mice were fed the different diets as described in methods. At week 8 on the corresponding diets the following parameters were measured in colon: **A-** PI3K protein levels and Akt phosphorylation (Ser473). **B–** NF-κB activation was evaluated measuring the phosphorylation of IKK (Ser176/180) and p65 (Ser536), **C-** MAPK activation was evaluated by measuring the phosphorylation of p38 (Thr180/Tyr182), ERK1/2 (Thr202/Tyr204), and JNK1/2 (Thr183/Tyr185). Bands were quantified and values for PI3K referred to HSC-70 levels (loading control) or for Akt, IKK, p65, p38, ERK1/2, JNK1/2 to total protein levels. All results for CA, HF and HFA were referred to control group values (C). Results are shown as mean ± SE of 9–10 animals/group. *Significantly different compared to all other groups ($p < 0.05$, one-way ANOVA test).

they were significantly higher (48% compared to C) than in all other groups (Fig. 7F).

4. Discussion

Four-week supplementation with cyanidin and delphinidin reverted or mitigated HFD-induced alterations in parameters of colon permeability, redox homeostasis and immune defenses. The beneficial actions of these AC protecting the intestinal barrier against fat-induced damage are largely mediated through TLR-4- and redox-regulated mechanisms. In the colon, consumption of the HFD caused disruption of TJs structure and function. This was associated with NOX1 and TLR-4 overexpression, and the consequent redox- and TLR-4-regulated activation of signaling pathways that modulate TJ opening, i.e. NF-κB, PI3K/Akt, ERK1/2 and JNK1/2. All these events were prevented or reverted by 4-week CDRE supplementation. Ensuing mechanistic studies in Caco-2 cells challenged with LPS support the actions of cyanidin and delphinidin and their major microbiota metabolites protecting the monolayer from permeabilization and modulating redox homeostasis and redox- and TLR-4-regulated signaling. Additionally, the HFD also affected the number and function of colonic goblet cells, changes that were reverted by CDRE supplementation.

Previous [21] and current findings show the development of metabolic endotoxemia between weeks 4 and 8 on the HFD. In support of the involvement of endotoxemia in HFD-associated colonic dysfunction, TLR-4 levels and downstream signaling cascades [20], i.e. NF-κB (IKK, p65), the MAPKs ERK1/2 and JNK1/2, and the PI3K/Akt pathway, were upregulated after 8 weeks on the HFD. The inhibition of the whole sequence of events (endotoxemia, activation of TLR-4 and downstream signaling) by CDRE supplementation stresses the potential relevance of dietary cyanidin and delphinidin in breaking the progression of high fat-mediated disruption of colonic barrier function and immune homeostasis. On the other hand, involvement of other mechanisms than those triggered by endotoxemia is evidenced by findings that while activation of signaling pathways downstream TLR-4 were observed after 8-week consumption of HFD, TJ protein levels and the number of goblet cells were already reduced after 4 weeks on the HFD. The latter could be in part due to the luminal increase of bile acids [6]. In this regard, deoxycholic acid promotes Caco-2 cell monolayer permeabilization through an increased oxidant production by mitochondria and NADPH oxidases, and the associated activation of redox signaling [30]. Overall, further research is necessary to understand the pathophysiology of the early damage of HFD on barrier integrity and goblet cell alterations and the mechanisms underlying AC protective actions.

The intestinal barrier function is sustained by TJs, which limit the passage of molecules, other than water and ions, in between epithelial cells. We observed alterations in colon barrier structure after 4 weeks consumption of the HFD, as evidenced by a decreased content of major TJ protein structural components, i.e. occludin, ZO-1 and claudin-1. After 8 weeks, other events involved in TJ opening were affected: i) activation of TJ regulatory signaling cascades, i.e. NF-κB, ERK1/2, Akt, and ii) increased MLCK expression and increased phosphorylation of

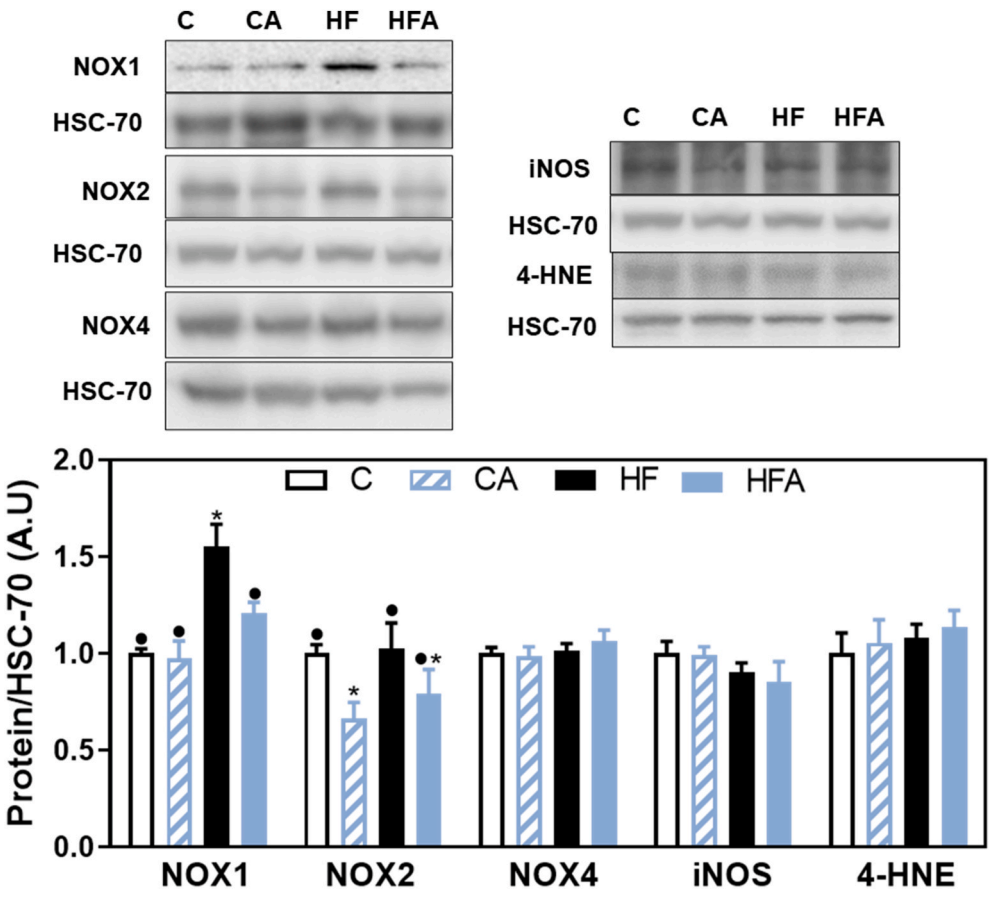

Fig. 6. Effects of supplementation with CDRE on parameters of colon oxidative stress and inflammation in mice fed a HFD. Mice were fed the different diets as described in methods. At week 8 on the corresponding diets the following parameters were measured in colon by Western blot: NOX1, gp91phox (NOX2), NOX4, iNOS and 4-HNE-protein adducts. Bands were quantified and values referred to HSC-70 levels (loading control). Results for CA, HF and HFA were referred to control group values (C). Results are shown as mean ± SE of 9–10 animals/group. Values having different symbols are significantly different ($p < 0.05$, one-way ANOVA test).

MLC, which causes the contraction of the actomyosin ring [31]. CDRE supplementation restored all the barrier parameters altered by the HFD, and also the mentioned downstream events. In Caco-2 cell monolayers, cyanidin and delphinidin, assayed as *O*-glucosides, and their microbiota metabolites, GA and PCA, prevented LPS-induced permeabilization. These results support that cyanidin and delphinidin, rather than other minor components in the CDRE, are the bioactives responsible of the protection of the colon epithelial barrier from HFD-mediated disruption.

The capacity of cyanidin and delphinidin to inhibit redox- and TLR-4-regulated signaling (NF-κB, MAPK, PI3K/Akt) can be involved in their actions preventing or restoring fat- and LPS-mediated alterations of barrier structure and function. In terms of TJ dynamics, phosphorylation of MLC by MLCK leads to the contraction of the perijunctional actomyosin ring with subsequent TJ opening. This can be also caused by the inhibitory phosphorylation of MLC phosphatase (MYPT-1) and subsequent increase in MLC phosphorylation. NF-κB, MAPK and PI3K/Akt regulate different events associated to TJ dynamics. In this regard, NF-κB [32,33] and ERK1/2 [34] promote MLCK gene transcription, NF-κB also regulates the expression and junctional localization of ZO-1 [32], and ERK1/2 phosphorylates and inactivates MYPT-1 [35,36]. JNK1/2 activation indirectly causes barrier disruption [37] *via* its proinflammatory actions [38]. Activation of the PI3K/Akt pathway causes barrier permeabilization [39,40], in part by downregulating claudin-1 expression [41], and increasing the expression of the pore-forming claudin-2 [40]. Mechanistically, observations in mice and Caco-2 cells were different, while in both models MLC phosphorylation was increased, in HFD mice this was mainly driven by MLCK overexpression, while in cells it was driven by MYPT-1 inactivation. This further supports the concept that additional mechanisms, to those mediated by LPS/TLR-4, are involved in HFD-induced loss of barrier function.

Exposure to high fat levels affects GI tract redox homeostasis in part through NOX1 upregulation. While distributed along the GI tract, NOX1 is expressed in large amounts in the epithelial cells of the colon [42]. NOX1 is a major player in sustaining GI tract physiology, but its overactivation is also associated to pathology. In this regard, animal models of colitis-associated neoplasia show increased expression of NOX1 [43]. TLR-4 and NOX1 transcripts are both upregulated in patients with Crohn's disease and colorectal cancer [43], suggesting a link between TLR-4 upregulation and NOX1 overexpression in human GI diseases. In fact, in response to the luminal microbiota, activation of TLR-4 leads to NOX1 transcription in part driven by NF-κB [44]. Supporting this link, we observed that HFD consumption upregulated both TLR-4 and NOX1. In this scenario, the capacity of the CDRE to suppress TLR-4/NF-κB/NOX1 upregulation could be considered of value to restore colon redox homeostasis and barrier function. On the other hand, while LPS did not cause an increase in NOX1 protein levels in Caco-2 cells, it did cause an increase in oxidant production and 4-HNE levels that were prevented by cyanidin, GA, PCA and/or delphinidin. Discrepancies in NOX1 expression between mice and cells are probably due to the different levels of complexity in the models. Nevertheless, both models show evidence of a disruption in redox homeostasis that was mitigated by AC.

Consumption of HFDs also affects goblet cells, other major component of the colonic immune system. Thus, HFD decreases the number of goblet cells and goblet cell proliferation in mouse colon [12,45,46]. HFD consumption for 4 weeks decreased the goblet cell population, while at 8 weeks it also reduced the mRNA levels of proteins produced by these cells, i.e. Klf4, involved in goblet cell differentiation; and Tff3, a regulator of mucus viscosity and mucosal healing. CDRE supplementation not only restored the levels of these proteins, but in the case of Tff3, it increased mRNA levels above control values. The latter effects could be due to AC helping in the repair of HFD-induced colonic mucosa damage. Thus, Tff3 is essential for mucosal restitution, regulating the rapid migration of the surface epithelium over the basement membrane [47].

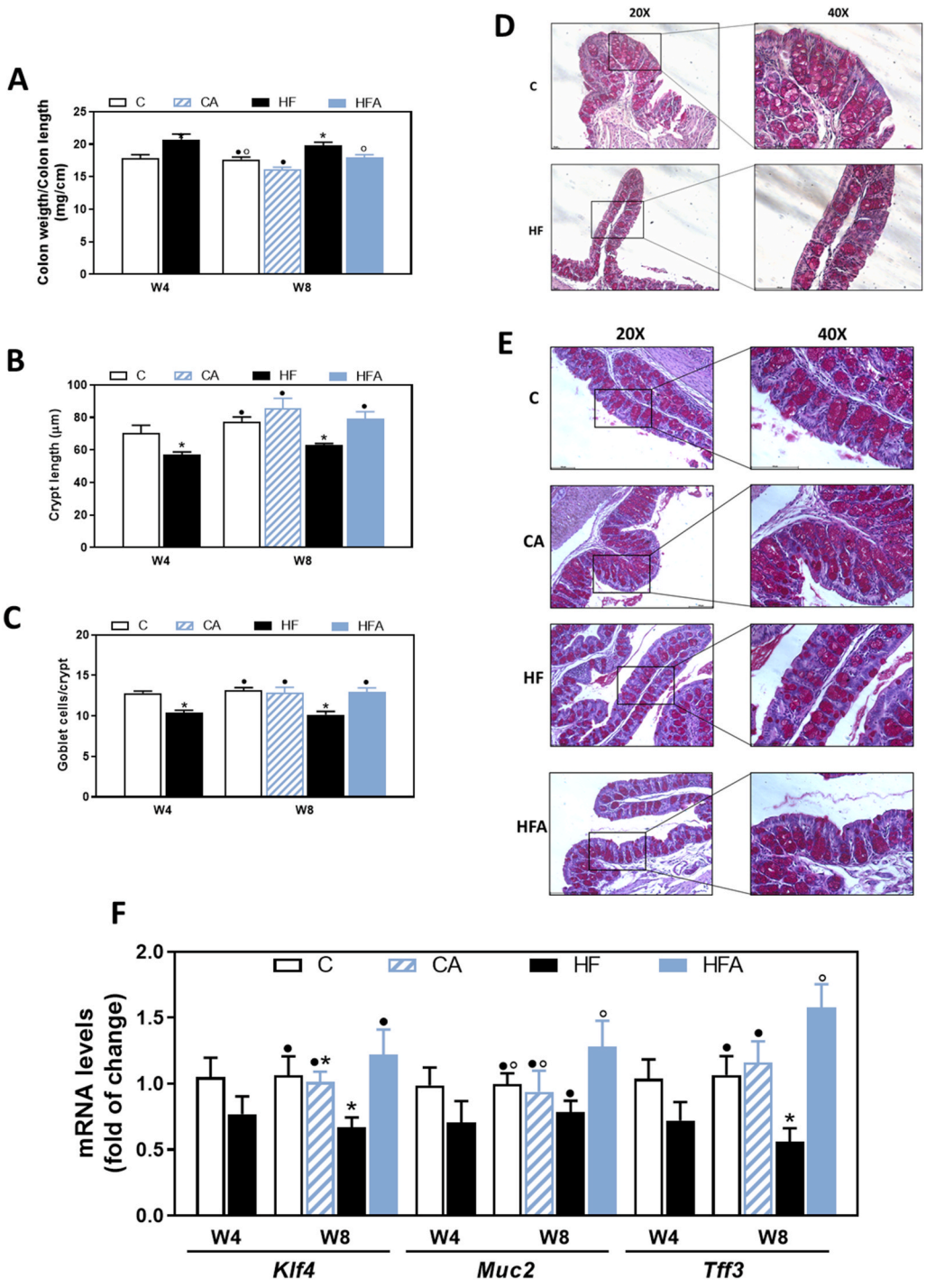

Fig. 7. Effects of the supplementation with CDRE on HFD-induced alterations in colon structure and goblet cells number and function. Mice were fed the different diets as described in methods. The following parameters were measured after 4 and/or 8 weeks on the corresponding treatments: **A**-colon weight/colon length, **B**- crypts length, **C**- goblet cells count, **D**-images of colon Periodic Acid Schiff (PAS) tissue staining at 4 weeks, and **E**-images of colon Periodic Acid Schiff (PAS) tissue staining at 8 weeks. **F**- Genes involved in goblet cells differentiation, i.e. Klf4, Muc2 and Tff3, were evaluated at 4 and 8 weeks on the dietary treatments by qPCR and values were normalized to 18S (housekeeping gene). **F**- Results for CA, HF and HFA were referred to control group values (C). Results are shown as mean ± SE of 6–9 animals/group. Values having different superscripts are significantly different ($p < 0.05$, one-way ANOVA test).

In the presence of inflammation or epithelial injury, Tff3 also promotes repair of the GI mucosa [48]. Overall, AC beneficial actions on goblet cell number and function are highly relevant to counteract the adverse consequence of HFD on the GI immune system.

5. Conclusions

In summary, the CDRE prevented or reverted HFD-induced alterations in colon structure, barrier integrity and goblet cell number and differentiation (Fig. 8). I*n vivo* and *in vitro* evidence support the actions of cyanidin and delphinidin mitigating TLR-4-activation, NOX1 upregulation, and loss of redox homeostasis. Additionally, CDRE supplementation also reverted the alterations in TJ structure that precedes endotoxemia. Overall, consumption of diets rich in AC, especially in cyanidin and delphinidin, can afford protection against the damage to the colon caused by the intake of diets rich in fats.

Author contributions

E.C. and D.E.I. ran all the experiments. P.I.O. designed the study. P.I.O., C.G.F, E.C. and D.E.I. wrote the manuscript. All authors revised the article, critically reviewed it for intellectual content, and approved the final version.

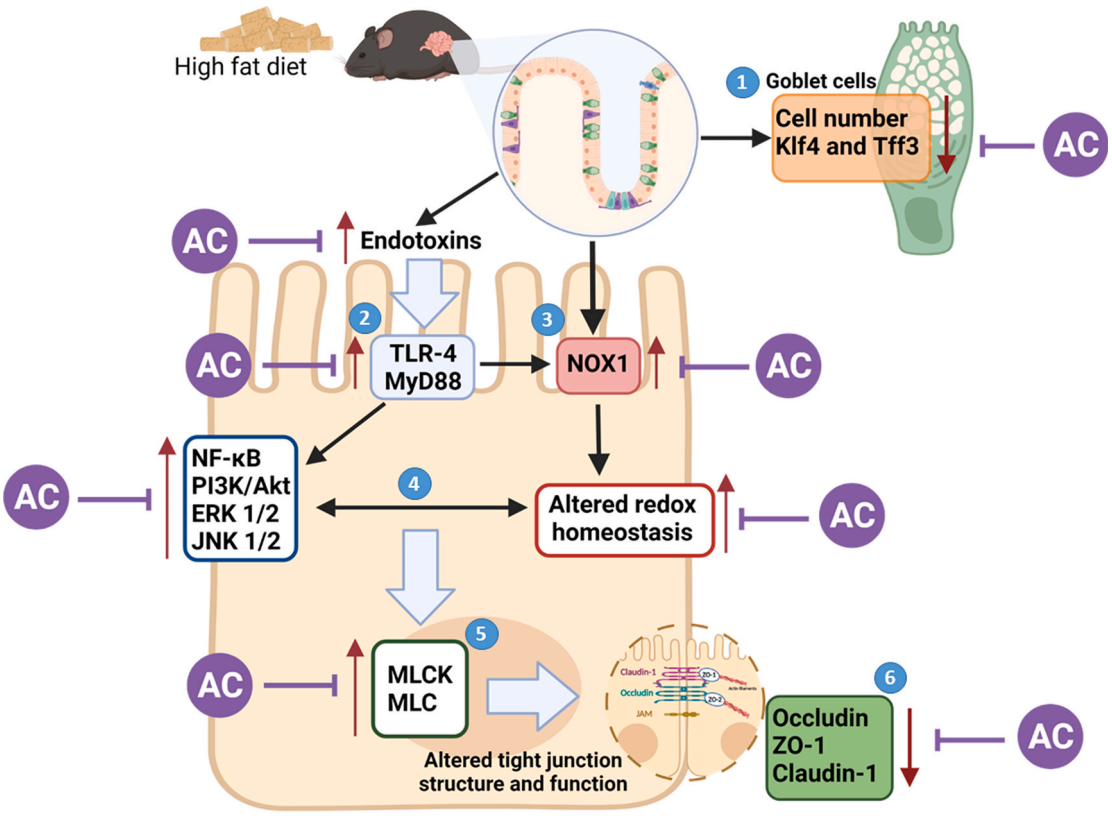

Fig. 8. Summary of results. Consumption of the HFD led to endotoxemia and alterations in colon physiology. In the colon we observed: ① a decrease in goblet cell number and alterations in parameters of goblet cell differentiation and function, including a downregulation of Klf4 and Tff3; ② increased TLR-4 and MyD88 expression; ③ increased NADPH oxidase NOX1 expression; ④ activation of redox-sensitive and TLR-4-triggered pathways, i.e. NF-κB, ERK1/2, JNK1/2, PI3K/Akt and ⑤⑥ disruption of tight junction function (activation of MLC) and structure, i.e. decreases in occludin, ZO-1 and claudin-1 protein levels. All these events were prevented or reverted by AC supplementation.

Declaration of competing interest

S.M.W., S.N.H. and M.B. are employed by Pharmanex Research, NSE Products Inc., Provo, UT, USA, the company that provided the test mix and research funding. C.G.F. and P.I.O. have received research grants from NSE Products Inc. C.G.F. and P.I.O. are members of the NSE Products Inc. Scientific Advisory Board. C.G.F. and P.I.O. have received research grants from other food companies and government agencies with an interest in health and nutrition.

Acknowledgements

Funding was provided by a research grant from Pharmanex Research, NSE Products Inc., Provo, UT, USA. PIO is correspondent researcher from CONICET, Argentina. The graphical abstract, Figs. 1A and 8 were generated using BioRender.com.

Appendix A. Supplementary data

Supplementary data to this article can be found online at https://doi.org/10.1016/j.freeradbiomed.2022.06.006.

References

[1] L. Geurts, A.M. Neyrinck, N.M. Delzenne, C. Knauf, P.D. Cani, Gut microbiota controls adipose tissue expansion, gut barrier and glucose metabolism: novel insights into molecular targets and interventions using prebiotics, Benef. Microbes 5 (2014) 3–17, https://doi.org/10.3920/BM2012.0065.

[2] J. Tomas, C. Mulet, A. Saffarian, J.B. Cavin, R. Ducroc, B. Regnault, C. Kun Tan, K. Duszka, R. Burcelin, W. Wahli, P.J. Sansonetti, T. Pedron, High-fat diet modifies the PPAR-gamma pathway leading to disruption of microbial and physiological ecosystem in murine small intestine, Proc. Natl. Acad. Sci. U.S.A 113 (2016) E5934–E5943, https://doi.org/10.1073/pnas.1612559113.

[3] T. Suzuki, H. Hara, Dietary fat and bile juice, but not obesity, are responsible for the increase in small intestinal permeability induced through the suppression of tight junction protein expression in LETO and OLETF rats, Nutr. Metab. 7 (2010) 19, https://doi.org/10.1186/1743-7075-7-19.

[4] E. Cremonini, E. Daveri, A. Mastaloudis, A.M. Adamo, D. Mills, K. Kalanetra, S. N. Hester, S.M. Wood, C.G. Fraga, P.I. Oteiza, Anthocyanins protect the gastrointestinal tract from high fat diet-induced alterations in redox signaling, barrier integrity and dysbiosis, Redox Biol. 26 (2019), 101269, https://doi.org/10.1016/j.redox.2019.101269.

[5] E. Cremonini, Z. Wang, A. Bettaieb, A.M. Adamo, E. Daveri, D.A. Mills, K. M. Kalanetra, F.G. Haj, S. Karakas, P.I. Oteiza, (-)-Epicatechin protects the intestinal barrier from high fat diet-induced permeabilization: implications for steatosis and insulin resistance, Redox Biol. 14 (2018) 588–599, https://doi.org/10.1016/j.redox.2017.11.002.

[6] M.W. Rohr, C.A. Narasimhulu, T.A. Rudeski-Rohr, S. Parthasarathy, Negative effects of a high-fat diet on intestinal permeability: a review, Adv. Nutr. 11 (2020) 77–91, https://doi.org/10.1093/advances/nmz061.

[7] E. Daveri, E. Cremonini, A. Mastaloudis, S.N. Hester, S.M. Wood, A.L. Waterhouse, M. Anderson, C.G. Fraga, P.I. Oteiza, Cyanidin and delphinidin modulate inflammation and altered redox signaling improving insulin resistance in high fat-fed mice, Redox Biol. 18 (2018) 16–24, https://doi.org/10.1016/j.redox.2018.05.012.

[8] M.A. Odenwald, J.R. Turner, The intestinal epithelial barrier: a therapeutic target? Nat. Rev. Gastroenterol. Hepatol. 14 (2017) 9–21, https://doi.org/10.1038/nrgastro.2016.169.

[9] P.D. Cani, J. Amar, M.A. Iglesias, M. Poggi, C. Knauf, D. Bastelica, A.M. Neyrinck, F. Fava, K.M. Tuohy, C. Chabo, A. Waget, E. Delmee, B. Cousin, T. Sulpice, B. Chamontin, J. Ferrieres, J.F. Tanti, G.R. Gibson, L. Casteilla, N.M. Delzenne, M. C. Alessi, R. Burcelin, Metabolic endotoxemia initiates obesity and insulin resistance, Diabetes 56 (2007) 1761–1772, https://doi.org/10.2337/db06-1491.

[10] E. Cremonini, A. Mastaloudis, S.N. Hester, S.V. Verstraeten, M. Anderson, S. M. Wood, A.L. Waterhouse, C.G. Fraga, P.I. Oteiza, Anthocyanins inhibit tumor necrosis alpha-induced loss of Caco-2 cell barrier integrity, Food Funct. 8 (2017) 2915–2923, https://doi.org/10.1039/c7fo00625j.

[11] D.E. Iglesias, E. Cremonini, C.G. Fraga, P.I. Oteiza, Ellagic acid protects Caco-2 cell monolayers against inflammation-induced permeabilization, Free Radic. Biol. Med. 152 (2020) 776–786, https://doi.org/10.1016/j.freeradbiomed.2020.01.022.

[12] M. Gulhane, L. Murray, R. Lourie, H. Tong, Y.H. Sheng, R. Wang, A. Kang, V. Schreiber, K.Y. Wong, G. Magor, S. Denman, J. Begun, T.H. Florin, A. Perkins, P. Cuív, M.A. McGuckin, S.Z. Hasnain, High fat diets induce colonic epithelial cell stress and inflammation that is reversed by IL-22, Sci. Rep. 6 (2016), 28990, https://doi.org/10.1038/srep28990.
[13] K.A. Knoop, R.D. Newberry, Goblet cells: multifaceted players in immunity at mucosal surfaces, Mucosal Immunol. 11 (2018) 1551–1557, https://doi.org/10.1038/s41385-018-0039-y.
[14] P.I. Oteiza, C.G. Fraga, D.A. Mills, D.H. Taft, Flavonoids and the gastrointestinal tract: local and systemic effects, Mol. Aspect. Med. 61 (2018) 41–49, https://doi.org/10.1016/j.mam.2018.01.001.
[15] A. Olejnik, K. Kowalska, M. Kidon, J. Czapski, J. Rychlik, M. Olkowicz, R. Dembczynski, Purple carrot anthocyanins suppress lipopolysaccharide-induced inflammation in the co-culture of intestinal Caco-2 and macrophage RAW264.7 cells, Food Funct. 7 (2016) 557–564, https://doi.org/10.1039/c5fo00890e.
[16] M. Ershad, M.K. Shigenaga, B. Bandy, Differential protection by anthocyanin-rich bilberry extract and resveratrol against lipid micelle-induced oxidative stress and monolayer permeability in Caco-2 intestinal epithelial cells, Food Funct. 12 (2021) 2950–2961, https://doi.org/10.1039/d0fo02377a.
[17] M.A. Polewski, D. Esquivel-Alvarado, N.S. Wedde, C.G. Kruger, J.D. Reed, Isolation and characterization of blueberry polyphenolic components and their effects on gut barrier dysfunction, J. Agric. Food Chem. (2020) 2940–2947, https://doi.org/10.1021/acs.jafc.9b01689.
[18] T. Le Phuong Nguyen, F. Fenyvesi, J. Remenyik, J.R. Homoki, P. Gogolák, I. Bácskay, P. Fehér, Z. Ujhelyi, G. Vasvári, M. Vecsernyés, J. Váradi, Protective effect of pure sour cherry anthocyanin extract on cytokine-induced inflammatory caco-2 monolayers, Nutrients 10 (2018) 861, https://doi.org/10.3390/nu10070861.
[19] B. Tian, J. Zhao, M. Zhang, Z. Chen, Q. Ma, H. Liu, C. Nie, Z. Zhang, W. An, J. Li, Lycium ruthenicum anthocyanins attenuate high-fat diet-induced colonic barrier dysfunction and inflammation in mice by modulating the gut microbiota, Mol. Nutr. Food Res. 65 (2021), e2000745, https://doi.org/10.1002/mnfr.202000745.
[20] S. Li, B. Wu, W. Fu, L. Reddivari, The anti-inflammatory effects of dietary anthocyanins against ulcerative colitis, Int. J. Mol. Sci. 20 (2019) 2588, https://doi.org/10.3390/ijms20102588.
[21] E. Cremonini, D.E. Iglesias, K.E. Matsukuma, S.N. Hester, S.M. Wood, M. Bartlett, C.G. Fraga, P.I. Oteiza, Supplementation with cyanidin and delphinidin mitigates high fat diet-induced endotoxemia and associated liver inflammation in mice, Food Funct. 13 (2022) 781–794, https://doi.org/10.1039/d1fo03108b.
[22] J. Kang, Z. Wang, P.I. Oteiza, (-)-Epicatechin mitigates high fat diet-induced neuroinflammation and altered behavior in mice, Food Funct. 11 (2020) 5065–5076, https://doi.org/10.1039/d0fo00486c.
[23] A. Bettaieb, M.A. Vazquez-Prieto, C.R. Lanzi, R.M. Miatello, F.G. Haj, C.G. Fraga, P. I. Oteiza, (-)-Epicatechin mitigates high fructose-associated insulin resistance by modulating redox signaling and endoplasmic reticulum stress, Free Radic. Biol. Med. 72 (2014) 247–256, https://doi.org/10.1016/j.freeradbiomed.2014.04.011.
[24] X. Rao, X. Huang, Z. Zhou, X. Lin, An improvement of the 2ˆ(-delta delta CT) method for quantitative real-time polymerase chain reaction data analysis, Biostat. Bioinforma. Biomath. 3 (2013) 71–85.
[25] A. Wojtala, M. Bonora, D. Malinska, P. Pinton, J. Duszynski, M.R. Wieckowski, Methods to monitor ROS production by fluorescence microscopy and fluorometry, Methods Enzymol. 542 (2014) 243–262, https://doi.org/10.1016/B978-0-12-416618-9.00013-3.
[26] C. Czank, A. Cassidy, Q. Zhang, D.J. Morrison, T. Preston, P.A. Kroon, N.P. Botting, C.D. Kay, Human metabolism and elimination of the anthocyanin, cyanidin-3-glucoside: a (13)C-tracer study, Am. J. Clin. Nutr. 97 (2013) 995–1003, https://doi.org/10.3945/ajcn.112.049247.
[27] P. Vitaglione, G. Donnarumma, A. Napolitano, F. Galvano, A. Gallo, L. Scalfi, V. Fogliano, Protocatechuic acid is the major human metabolite of cyanidin-glucosides, J. Nutr. 137 (2007) 2043–2048, https://doi.org/10.1093/jn/137.9.2043.
[28] Z. Racova, E. Anzenbacherova, B. Papouskova, S. Poschner, P. Kucova, J. C. Gausterer, F. Gabor, M. Kolar, P. Anzenbacher, Metabolite profiling of natural substances in human: in vitro study from fecal bacteria to colon carcinoma cells (Caco-2), J. Nutr. Biochem. 85 (2020), 108482, https://doi.org/10.1016/j.jnutbio.2020.108482.
[29] K. Kahle, M. Kraus, W. Scheppach, M. Ackermann, F. Ridder, E. Richling, Studies on apple and blueberry fruit constituents: do the polyphenols reach the colon after ingestion? Mol. Nutr. Food Res. 50 (2006) 418–423, https://doi.org/10.1002/mnfr.200500211.
[30] Z. Wang, M.C. Litterio, M. Muller, D. Vauzour, P.I. Oteiza, (-)-Epicatechin and NADPH oxidase inhibitors prevent bile acid-induced Caco-2 monolayer permeabilization through ERK1/2 modulation, Redox Biol. 28 (2020), 101360, https://doi.org/10.1016/j.redox.2019.101360.
[31] K.E. Cunningham, J.R. Turner, Myosin light chain kinase: pulling the strings of epithelial tight junction function, Ann. N. Y. Acad. Sci. 1258 (2012) 34–42, https://doi.org/10.1111/j.1749-6632.2012.06526.x.
[32] T.Y. Ma, G.K. Iwamoto, N.T. Hoa, V. Akotia, A. Pedram, M.A. Boivin, H.M. Said, TNF-alpha-induced increase in intestinal epithelial tight junction permeability requires NF-kappa B activation, Am. J. Physiol. Gastrointest. Liver Physiol. 286 (2004) G367–G376, https://doi.org/10.1152/ajpgi.00173.2003286/3/G367 [pii]:.
[33] D. Ye, T.Y. Ma, Cellular and molecular mechanisms that mediate basal and tumour necrosis factor-alpha-induced regulation of myosin light chain kinase gene activity, J. Cell Mol. Med. 12 (2008) 1331–1346. JCMM302 [pii]10.1111/j.1582-4934.2008.00302.x.
[34] R. Al-Sadi, S. Guo, D. Ye, T.Y. Ma, TNF-alpha modulation of intestinal epithelial tight junction barrier is regulated by ERK1/2 activation of Elk-1, Am. J. Pathol. 183 (2013) 1871–1884, https://doi.org/10.1016/j.ajpath.2013.09.001S0002-9440(13)00601-9 [pii]:.
[35] D. Xiao, L.D. Longo, L. Zhang, Alpha1-adrenoceptor-mediated phosphorylation of MYPT-1 and CPI-17 in the uterine artery: role of ERK/PKC, Am. J. Physiol. Heart Circ. Physiol. 288 (2005) H2828–H2835, https://doi.org/10.1152/ajpheart.01189.2004.
[36] E. Ihara, Q. Yu, M. Chappellaz, J.A. MacDonald, ERK and p38MAPK pathways regulate myosin light chain phosphatase and contribute to Ca2+ sensitization of intestinal smooth muscle contraction, Neuro Gastroenterol. Motil. 27 (2015) 135–146, https://doi.org/10.1111/nmo.12491.
[37] J. Zhou, M. Boutros, JNK-dependent intestinal barrier failure disrupts host-microbe homeostasis during tumorigenesis, Proc. Natl. Acad. Sci. U.S.A 117 (2020) 9401–9412, https://doi.org/10.1073/pnas.1913976117.
[38] A.D. Mandić, E. Bennek, J. Verdier, K. Zhang, S. Roubrocks, R.J. Davis, B. Denecke, N. Gassler, K. Streetz, A. Kel, M. Hornef, F.J. Cubero, C. Trautwein, G. Sellge, c-Jun N-terminal kinase 2 promotes enterocyte survival and goblet cell differentiation in the inflamed intestine, Mucosal Immunol. 10 (2017) 1211–1223, https://doi.org/10.1038/mi.2016.125.
[39] M. Amasheh, A. Fromm, S.M. Krug, S. Amasheh, S. Andres, M. Zeitz, M. Fromm, J. D. Schulzke, TNFalpha-induced and berberine-antagonized tight junction barrier impairment via tyrosine kinase, Akt and NFkappaB signaling, J. Cell Sci. 123 (2010) 4145–4155, https://doi.org/10.1242/jcs.070896.
[40] T. Suzuki, N. Yoshinaga, S. Tanabe, Interleukin-6 (IL-6) regulates claudin-2 expression and tight junction permeability in intestinal epithelium, J. Biol. Chem. 286 (2011) 31263–31271, https://doi.org/10.1074/jbc.M111.238147M111.238147 [pii]:.
[41] N. Khan, L. Binder, D.V.K. Pantakani, A.R. Asif, MPA modulates tight junctions' permeability via midkine/PI3K pathway in caco-2 cells: a possible mechanism of leak-flux diarrhea in organ transplanted patients, Front. Physiol. 8 (2017) 438, https://doi.org/10.3389/fphys.2017.00438.
[42] I. Szanto, L. Rubbia-Brandt, P. Kiss, K. Steger, B. Banfi, E. Kovari, F. Herrmann, A. Hadengue, K.H. Krause, Expression of NOX1, a superoxide-generating NADPH oxidase, in colon cancer and inflammatory bowel disease, J. Pathol. 207 (2005) 164–176, https://doi.org/10.1002/path.1824.
[43] J.F. Burgueno, J. Fritsch, E.E. Gonzalez, K.S. Landau, A.M. Santander, I. Fernandez, H. Hazime, J.M. Davies, R. Santaolalla, M.C. Phillips, S. Diaz, R. Dheer, N. Brito, J. Pignac-Kobinger, E. Fernandez, G.E. Conner, M.T. Abreu, Epithelial TLR4 signaling activates DUOX2 to induce microbiota-driven tumorigenesis, Gastroenterology 160 (2021) 797–808, https://doi.org/10.1053/j.gastro.2020.10.031, e6.
[44] S. van der Post, G.M.H. Birchenough, J.M. Held, NOX1-dependent redox signaling potentiates colonic stem cell proliferation to adapt to the intestinal microbiota by linking EGFR and TLR activation, Cell Rep. 35 (2021) 108949, https://doi.org/10.1016/j.celrep.2021.108949.
[45] Y. Xie, F. Ding, W. Di, Y. Lv, F. Xia, Y. Sheng, J. Yu, G. Ding, Impact of a highfat diet on intestinal stem cells and epithelial barrier function in middleaged female mice, Mol. Med. Rep. 21 (2020) 1133–1144, https://doi.org/10.3892/mmr.2020.10932.
[46] C.H. Dinh, Y. Yu, A. Szabo, Q. Zhang, P. Zhang, X.F. Huang, Bardoxolone methyl prevents high-fat diet-induced colon inflammation in mice, J. Histochem. Cytochem. 64 (2016) 237–255, https://doi.org/10.1369/0022155416631803.
[47] H. Mashimo, D.C. Wu, D.K. Podolsky, M.C. Fishman, Impaired defense of intestinal mucosa in mice lacking intestinal trefoil factor, Science 274 (1996) 262–265, https://doi.org/10.1126/science.274.5285.262.
[48] D. Taupin, D.K. Podolsky, Trefoil factors: initiators of mucosal healing, Nat. Rev. Mol. Cell Biol. 4 (2003) 721–732, https://doi.org/10.1038/nrm1203.